The Generation of Axial Multiplane Optical Angular Momentum Based on Liquid Crystal Device

Heng Li, Peng Shi, Luping Du, Wanlong Zhang, Cong Liu, Xinxin Gou, Xiaocong Yuan*

Nanophotonics Research Centre, Shenzhen Key Laboratory of Micro-Scale Optical Information Technology, Institute of Micro/Nano Optoelectronics, Shenzhen University, 518060, China

ABSTRACT

The demand for high capacity and integration in modern optical communication technology is becoming prominent. Orbital angular momentum (OAM) plays an important role in optical communication. However, there are still challenges to further expand the flexibility and capacity of optical communication in the axial direction. Here, we propose a single-layer liquid crystal device (LCD) to realize the generation of optical vortex (OV) array with arbitrary topological charge in axial multiplane, which can be applied in optical communications based on highly integrated device.

The phase of the target OV array is weighted and superimposed to obtain the phase distribution of LCD. In order to obtain an OV array with uniform intensity, it is necessary to determine the optimal weight factor for each OV based on the introduced particle swarm optimization (PSO) algorithm.

In the experiment, a LCD with an effective aperture of 2 mm was processed. A CCD captures the OV array image, including two OV arrays at 200*λ (156μm) in front of and behind the focal point respectively. Then, the beam passes through the 4f system of the spatial light modulator with the phase distribution of the Damman vortex grating on the spectrum plane, and the topological charge of the two OV arrays can be detected by the CCD.

Our results provide an approach that based on a single liquid crystal plate, OV arrays in multiple propagation planes are realized, in which the number of propagation planes and the position of each propagation plane relative to the back focal plane can be adjusted arbitrarily, and the number, order, and position of OVs in each propagation plane can also be adjusted arbitrarily to meet the application requirements in the field of short-distance optical communication.

KEYWORDS: *Optical vortex array, Orbital angular momentum, Axial multiplane, Liquid crystal device, Optical vortex detection*

INTRODUCTION

Light has multiple degrees of freedom, including frequency, amplitude, phase, polarization, spin angular momentum (SAM) and orbital angular momentum (OAM). In 1992, OAM was first discovered in experiments by Allen et al.[1], and it was proved for the first time that each photon in an optical field with a vortex phase structure carries an orbital angular momentum of $l\hbar$, where l represents the helical quantum number of the phase. This optical field with vortex phase is called optical vortex (OV). The wavefront of OV wraps around the central phase singularity and propagates in a spiral shape, and forms a dark spot with zero light intensity in the center, making the light intensity present a doughnut-shaped distribution[2]. The microscopic OAM of photons is connected with the macroscopic intensity distribution of OV, which has made great progress in different fields of research on OAM in recent years.

As one of the degrees of freedom of light, OAM can boost the optical[3] and quantum[4] information capacity because of its theoretically infinite helical mode index[5]. Also, more and more researchers focus on OAM, mainly involving regulation and application. The ways to efficiently distinguish photons with different OAM[6][7] enable future demultiplexing processes utilizing OAM-encoded information. Study on the propagation characteristics[8][9][10] can be fundamental for free space communication. Researches of the application of photon OAM in the field of quantum information[11][12][13] is of great significance for understanding some basic problems of quantum mechanics by using the new degree of freedom of photons. Applications of OAM for precision measurement[14][15][16], sensing[17][18], imaging[19][20], and classical optical communication[21][22].Novel and efficient generation methods were introduced

SPIE-CLP Conference on Advanced Photonics 2022, edited by Xu Liu,
Anatoly Zayats, Xiaocong Yuan, Proc. of SPIE Vol. 12601, 126010H

for OAM, which include etching special structures on silicon substrates[23][24], surface plasmon excitation[25][26], spatial light modulator (SLM)[27], liquid crystal device (LCD)[28]. The OAM generation methods mentioned above cannot meet the requirements of high integration and OAM generation only on a specific plane at the same time.

In this work, we introduce a single LCD to generate OV arrays on specific propagation surfaces, where the order and position of OVs in the surfaces can be adjusted arbitrarily. First, we obtain the phase distribution of the LCD on the diffraction plane by weighting the superposition of the phase of the target OV arrays based on the vector diffraction theory. In this process, we introduce the particle swarm optimization (PSO) algorithm to obtain OV arrays with uniform intensity. Next, we fabricated a LCD with an effective working aperture of 2 mm to host the above phase plane, and its work wavelength is 780nm. Then, experimentally, we built an optical system to test the LCD. Specifically, a 780nm single-frequency laser is used as the light source; a combination of a half-wave plate and a quarter-wave plate is used to generate circularly polarized light as the incident light of the LCD; the CCD can directly detect the light intensity distribution of the OV arrays, the order of OVs can also be detected by the cooperation between SLM and 4f system.

Our study provides a way to generate arbitrarily tunable OV arrays on highly integrated devices. And the introduced OV arrays are only distributed on specific propagation surfaces, so the information they carries can only be read at specific positions, thus showing attractive potential in high speed and integrated optical encrypted communication.

DESIGN AND OPTIMIZATION OF LCD

To get the desired OV array at a specific location, we need to solve an inverse problem. That is, for the target field distribution, we find the corresponding incident field. Today, driven by the rapid development of computational electrodynamics, such inverse problems have attracted many interests[29][30]. And different algorithms have been developed in different application scenarios, for instance surface plasmon[31], three-dimensional vectorial holography[32], and Au nanostructure arrays[33]. In this work, we use vector diffraction integral based method together with the introduced PSO algorithm[34] to solve the problem.

As it's mentioned, the phase modulation of LCD is realized by superposing the phase of the target OV array. However, under the condition of the same weight superposition, in the OV array generated by the designed LCD, the intensity of low-order OVs will be higher than that of high-order OVs. In the PSO algorithm, multiple parameters are considered to obtain a meaningful OV array with a clear background, moderate intensity, and uniform intensity distribution among each OV. In more detail, we define a certain number of weight factor groups in a high-dimensional space, that is, particles in a certain range of values in the PSO algorithm. The particle swarm moves in this parameter space through a stochastic optimization process to find an optimal value of a defined merit function[34]. Obviously, this merit function needs to be carefully considered to ensure that the resulting OV array satisfies the requirements in many respects. In this work, all pixels of the image of the OV array will be read one by one to generate a merit function to evaluate the quality of the OV array. There are three key parameters of the merit function. Noise signal intensity, which is quantized as the number of pixels whose intensity is below a certain threshold. OV signal intensity, which is quantized as the number of pixels whose intensity is above a certain threshold. OV signal uniformity, which is quantified as the variance among the OV signal intensities in the OV array image. Here, we need to find the minimum value of the merit function, so when we superimpose the above three key parameters, we need to add a negative sign in front of the OV signal intensity.

The phase definition of the target OV array is relatively simple, only the position of each OV in polar coordinates and the topological charge of the OV need to be defined. After obtaining the phase of the target OV array and the weighting factors of each OV phase, the phase distribution of the LCD can be obtained based on the vector diffraction integral.

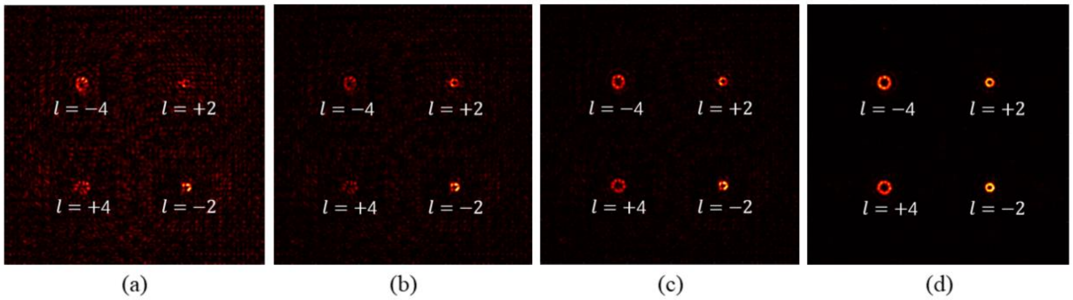

Figure 1. Schematic diagram of the optimization effect based on the PSO algorithm. The optimization results of OV array intensity distribution for 60 particles from (a) to (d) for 50, 100, 500 and 1000 iterations respectively. It can be seen that the noise of the OV array image is reduced, the signal is enhanced, and the intensity distribution of OV tends to be uniform

FABRICATION AND MEASUREMENT OF LCD

LCD mainly realizes the phase modulation of the incident beam through the birefringence of liquid crystal molecules. More specifically, changing the voltage applied to the liquid crystal pixel molecules, there will be different angles between the liquid crystal molecules and the electric field, that is, the director of the liquid crystal molecules and the polarization direction of the incident light form a certain angle, thus the liquid crystal effective refractive index is changed. The optical path also changes accordingly, so as to achieve the phase modulation. In this work, the LCD with a 2 mm effective aperture can work in an optical system with 780 nm incident light. The number of pixels of the aperture diameter is 1024, and the substrate material used is silicon dioxide.

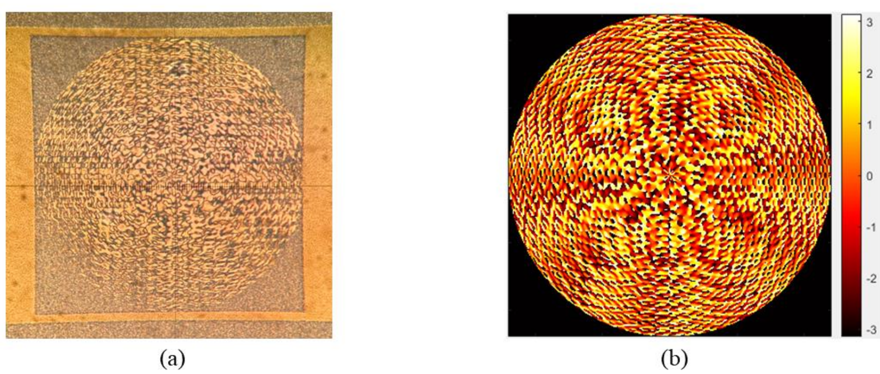

Figure 2. (a) Picture of LCD under polarization microscope, the working area of the LCD is a circle with a diameter of 2mm, (b) LCD phase distribution calculated based on vector diffraction theory.

Experimentally, we use a 780nm single-frequency laser as the light source, collimate the expanded beam, and filter the stray light with the diaphragm. Then let this beam pass through the linear polarizer, the quarter wave plate in turn, and reach the CCD. The light intensity of the OV array can then be measured directly. When it comes to the topological charge of the OV array, we introduce a 4f system in front of the CCD, where the SLM is placed on the spectrum plane. Taking the measurement of one of the OVs as an example, an OV with an order of +2 generated by the LCD via the SLM set a phase of a one-dimensional Damman vortex grating phase with an order of -2, and the intensity distribution of the OV can be observed on the CCD to become Gaussian distribution, that is, the order has become 0. By analogy, we can measure each OV one by one.

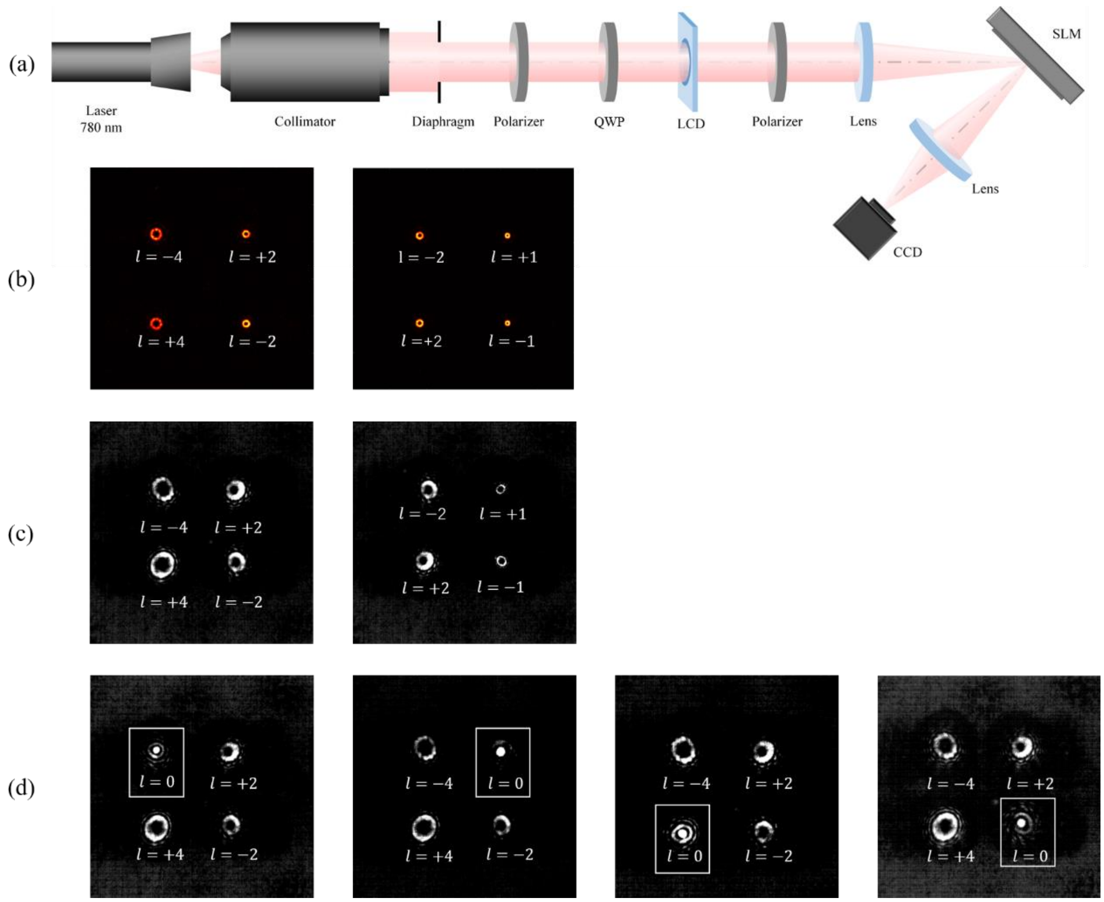

Figure 3. (a) Experimental setup to generate axial multiplanar OV arrays and test topological charges. Circularly polarized light with a wavelength of 780nm enters the LCD. (b) and (c) are the theoretical and experimental results of the OV array at a distance of 200λ before and after the focal point, respectively. By adjusting the SLM on the three-dimensional displacement stage to offset the OV of different orders in the axial direction and in the plane to make it a Gaussian point as shown in (d). QWP, quarter-wave plate; SLM, spatial light modulator.

CONCLUSION

In this work, we developed an LCD for realizing axial multiplane generation of OV arrays. The arrangement of the OV array in the plane and the distance of the axial multi-plane can be adjusted according to the actual application. This idea can be extended to apply this type of device to mass production based on metasurface and nanoimprinting technology, or to generate axial multiplanar OVs that vary in time domain based on tunable phase modulation devices, such as SLM, etc. The method has application prospects in the generation of OAM, OAM multiplexing of optical communication, and optical encrypted communication.

REFERENCE

[1] Allen, Les, et al. "Orbital angular momentum of light and the transformation of Laguerre-Gaussian laser modes." Physical review A 45.11 (1992): 8185.

[2] Desyatnikov, Anton S., Lluis Torner, and Yuri S. Kivshar. "Optical vortices and vortex solitons." arXiv preprint nlin/0501026 (2005).

[3] Wang, Jian, et al. "Terabit free-space data transmission employing orbital angular momentum multiplexing." Nature photonics 6.7 (2012): 488-496.

[4] Mair, Alois, et al. "Entanglement of the orbital angular momentum states of photons." Nature 412.6844 (2001): 313-316.
[5] Hemsing, E., A. Marinelli, and J. B. Rosenzweig. "Generating optical orbital angular momentum in a high-gain free-electron laser at the first harmonic." Physical Review Letters 106.16 (2011): 164803.
[6] Leach, Jonathan, et al. "Measuring the orbital angular momentum of a single photon." Physical review letters 88.25 (2002): 257901.
[7] Berkhout, Gregorius CG, et al. "Efficient sorting of orbital angular momentum states of light." Physical review letters 105.15 (2010): 153601.
[8] Krenn, Mario, et al. "Communication with spatially modulated light through turbulent air across Vienna." New Journal of Physics 16.11 (2014): 113028.
[9] Krenn, Mario, et al. "Twisted photon entanglement through turbulent air across Vienna." Proceedings of the National Academy of Sciences 112.46 (2015): 14197-14201.
[10] Krenn, Mario, et al. "Twisted light transmission over 143 km." Proceedings of the National Academy of Sciences 113.48 (2016): 13648-13653.
[11] Mair, Alois, et al. "Entanglement of the orbital angular momentum states of photons." Nature 412.6844 (2001): 313-316.
[12] Leach, Jonathan, et al. "Quantum correlations in optical angle–orbital angular momentum variables." Science 329.5992 (2010): 662-665.
[13] Fickler, Robert, et al. "Quantum entanglement of high angular momenta." Science 338.6107 (2012): 640-643.
[14] Lee, Jae Hoon, et al. "Experimental verification of an optical vortex coronagraph." Physical review letters 97.5 (2006): 053901.
[15] Kravets, V. G., et al. "Singular phase nano-optics in plasmonic metamaterials for label-free single-molecule detection." Nature materials 12.4 (2013): 304-309.
[16] Brullot, Ward, et al. "Resolving enantiomers using the optical angular momentum of twisted light." Science advances 2.3 (2016): e1501349.
[17] Wang, Wei, et al. "Optical vortex metrology for nanometric speckle displacement measurement." Optics express 14.1 (2006): 120-127.
[18] Lavery, Martin PJ, et al. "Detection of a spinning object using light's orbital angular momentum." Science 341.6145 (2013): 537-540.
[19] Chen, Lixiang, Jijin Lei, and Jacquiline Romero. "Quantum digital spiral imaging." Light: Science & Applications 3.3 (2014): e153-e153.
[20] Morris, Peter A., et al. "Imaging with a small number of photons." Nature communications 6.1 (2015): 1-6.
[21] Bozinovic, Nenad, et al. "Terabit-scale orbital angular momentum mode division multiplexing in fibers." science 340.6140 (2013): 1545-1548.
[22] Willner, Alan E., et al. "Optical communications using orbital angular momentum beams." Advances in optics and photonics 7.1 (2015): 66-106.
[23] Cai, Xinlun, et al. "Integrated compact optical vortex beam emitters." Science 338.6105 (2012): 363-366.
[24] Strain, Michael J., et al. "Fast electrical switching of orbital angular momentum modes using ultra-compact integrated vortex emitters." Nature communications 5.1 (2014): 1-7.
[25] Karimi, Ebrahim, et al. "Generating optical orbital angular momentum at visible wavelengths using a plasmonic metasurface." Light: Science & Applications 3.5 (2014): e167-e167.
[26] Mei, Shengtao, et al. "On-chip discrimination of orbital angular momentum of light with plasmonic nanoslits." Nanoscale 8.4 (2016): 2227-2233.
[27] Curtis, Jennifer E., Brian A. Koss, and David G. Grier. "Dynamic holographic optical tweezers." Optics communications 207.1-6 (2002): 169-175.
[28] Chen, Peng, et al. "Digitalizing self-assembled chiral superstructures for optical vortex processing." Advanced Materials 30.10 (2018): 1705865.
[29] Ren, Haoran, et al. "Three-dimensional vectorial holography based on machine learning inverse design." Science advances 6.16 (2020): eaaz4261.
[30] Bancerek, Maria, Krzysztof M. Czajkowski, and Rafał Kotyński. "Far-field signature of sub-wavelength microscopic objects." Optics Express 28.24 (2020): 36206-36218.
[31] Malkiel, Itzik, et al. "Plasmonic nanostructure design and characterization via deep learning." Light: Science & Applications 7.1 (2018): 1-8.

[32] Ren, Haoran, et al. "Three-dimensional vectorial holography based on machine learning inverse design." Science advances 6.16 (2020): eaaz4261.
[33] Volpe, Giorgio, Gabriel Molina-Terriza, and Romain Quidant. "Deterministic subwavelength control of light confinement in nanostructures." Physical review letters 105.21 (2010): 216802.
[34] Robinson, Jacob, and Yahya Rahmat-Samii. "Particle swarm optimization in electromagnetics." IEEE transactions on antennas and propagation 52.2 (2004): 397-407.